Clay Science 19, 45–51 (2015)

–Paper–

CRYSTAL GROWTH OF A HECTORITE-LIKE LAYERED SILICATE ON MONODISPERSE SPHERICAL SILICA PARTICLES WITH DIFFERENT DIAMETERS

TOMOHIKO OKADA* and ASUKA SUZUKI

Department of Chemistry and Material Engineering, Faculty of Engineering, Shinshu University, Wakasato 4-17-1, Nagano 380-8553, Japan

(Received May 11, 2015. Accepted June 13, 2015)

ABSTRACT

Fine crystals of hectorite-like layered silicate formed using hydrothermal reactions on monodisperse spherical silica particles with diameters of 0.2, 0.6 and 1.0 μm. The reactions were performed in a colloidal spherical silica suspension with lithium and magnesium ions under alkaline conditions at 373 K in a rotating Teflon-lined autoclave at the $LiF:MgCl_2:SiO_2$ molar ratio of 0.21:0.8:8.0. The grain size distributions were quite uniform irrespective of the silica size in the initial mixtures, as a result of the high rate of heterogeneous nucleation reaction than that of the homogeneous nucleation. The amount of a cationic surfactant that was intercalated tended to be large when the grain size of the silica spheres was small, while the negative layer charge of the hectorite-like silicate was same extent.

Key words: Colloidal silica, Heterogeneous nucleation, Layered silicate, Cation-exchange, Sacrificial template method

INTRODUCTION

The smectite group of layered clay minerals has been extensively studied the most widely owing to their cation exchange ability, large surface area, and chemical and thermal stability (Theng, 1974; van Olphen, 1977; Bergaya et al., 2006). The potentials for synthesis (Newmann and Sansom, 1970; Torii and Iwasaki, 1986; Nakazawa et al., 1992; Yamada et al., 1994; 1995; Tateyama et al., 1996; Kloprogge et al., 1999; Carrado et al., 1991; 1993; 1997; Carrado, 2000; Reinholdt et al., 2001; Ogawa et al., 2008; 2009) and surface modification (Lagaly, 1986; Mortlamd et al., 1986; Lagaly and Beneke; 1991; Ogawa and Kuroda, 1997; Takagi et al., 2006; Okada and Ogawa, 2010; Park et al., 2011; Okada et al., 2014) give smectites and their resulting hybrids with structural and compositional versatility. Cation-exchange reactions between the interlayer cations and organoammonium ions are well known, and they are used in such applications as modifying surfaces, producing hydrophobic and microporous inorganic–organic hybrids for the uptake of specific molecules (Barrer, 1989; Xu et al., 1997), producing controlled release materials, achieving selective catalysis and achieving efficient photo-induced processes (Okada et al., 2012; Takagi et al., 2013). On the other hand, the shapes required for the applications especially in photo/electro-functional materials have been produced through the bottom-up self-assembly of the silicate layers using optically transparent films (Ogawa et al., 1994; Sasai et al., 2004; Takagi et al., 2010; Kawamata et al., 2010) fabricated through various techniques (including depositing a smectite suspension on a substrate, using the Langmuir–Blodgett technique to exfoliate platelets (Inukai et al., 1994; Hotta et al., 1997; Suzuki et al., 2012)) and using a layer-by-layer deposition technique (Kleinfeld, E. R. and Ferguson, 1994; Lvov, et al., 1996; Lotsch and Ozin, 2008). The deposition of the silicate layers of smectites on different particles using an alternating adsorption technique (Hickey et al., 2011) has recently been reported as another class of multifunctional materials with hierarchical hybridizations to be produced.

We reported the *in situ* crystallization of a hectorite-like layered silicate (abbreviated to Hect) with the ideal formula $Li_x(Mg_{6-x}Li_xSi_8O_{20}(OH)_4)\cdot nH_2O$ on spherical silica particles (Okada et al., 2012b; Okada et al., 2015). In that process the silica particles were partially consumed through hydrothermal reactions without losing the silica morphology, and the dissolved silica was used as the source of Hect. The core-shell hybridization is not like the *papier mâché* method, but the so-called sacrificial template or self-template method, and it is

* Corresponding author: Tomohiko Okada, Department of Chemistry and Material Engineering, Faculty of Engineering, Shinshu University, Wakasato 4-17-1, Nagano 380-8553, Japan. e-mail: tomohiko@shinshu-u.ac.jp

possible to avoid flakes falling off the silica particles even in aqueous media. The monodisperse core-shell particles (abbreviated to Silica@Hect) produced using the sacrificial template method could be used as host materials and/or building units in future separation, sensor, optics and electronic applications because the periodic arrangement of smectite (or a related layered solid) particles with defined shapes is key to achieving more sophisticated functional materials (Ozin et al., 2009; Ariga et al., 2012). Here, we describe the effects of the grain size of initial spherical silicas (0.2, 0.6, and 1.0 μm) on the crystal growth of Hect using the sacrificial template method. In addition, the effects of the nature of the Li source (LiF and LiCl) in the starting mixtures are also discussed in this paper.

MATERIALS AND METHODS.

Materials

Lithium fluoride, lithium chloride, magnesium dichloride hexahydrate, urea, and dioctadecyldimethylammonium (abbreviated to $2C_{18}$) bromide were purchased from Wako Pure Chemical Ind., Ltd. Monodisperse spherical silicas with the grain sizes of 0.2 μm (HF–Silibol–S 200, Toyama Chemical Co., Ltd.), 0.6 μm (HPS–0500, Toagosei Co., Ltd.), and 1.0 μm (KE–S100, Nippon Shokubai Co., Ltd.) were used as the sources of Hect. All these chemicals were used without further purification.

Fabrication of Silica@Hect core-shell particles using different grain sizes of the spherical silicas

A typical procedure was reported in the previous paper (Okada, et al., 2015). The LiF:$MgCl_2$:SiO_2:urea molar ratio in the starting mixture was 0.21:0.8:8.0:8.0, where the layer charge density of the resulting Hect was low. Urea (2.16 g), $MgCl_2 \cdot 6H_2O$ (0.73 g) and LiF (0.024 g) were dissolved in water (80 mL). LiCl was also used instead of LiF. The resulting solution was mixed with an aqueous suspension of spherical silica particles (2.16 g in 20 mL of water) using a mechanical homogenizer (at 4600 revolutions per minute) for 30 min at room temperature. The slurry was transferred to a Teflon-lined autoclave and heated to 373 K for 48 h. The autoclave was rotated at 15 revolutions per minute using a hydrothermal synthesis reactor unit (Hiro Company) during the heat treatment. The slurry was then cooled in an ice bath and centrifuged (at 1400 g for 20 min), then the precipitate was collected and dried at 323 K. In the case of using LiCl, the precipitate was washed with water repeatedly before drying. In Table 1, the sample name is summarized.

Cation-exchange reactions of Silica@Hect with a cationic surfactant

$2C_{18}$ bromide (15 mg) in a mixture of water and ethanol (10 mL, 50/50 v/v) was allowed to react with Silica@Hect (0.1 g) by magnetic stirring at room temperature for 1 day. The product was collected by centrifugation (1400 g for 20 min); this was followed by repeated washing with the mixture of water and ethanol (50/50 *v/v*). Finally, the washed solid was dried at 323 K.

TABLE 1. Sample list in the present study.

grain size of the spherical silica [mm]	counter anion of Li salt used	sample name
0.2	F^-	Silica0.2@HectF
	Cl^-	Silica0.2@HectCl
0.6	F^-	Silica0.6@HectF
	Cl^-	Silica0.6@HectCl
1.0	F^-	Silica1.0@HectF
	Cl^-	Silica1.0@HectCl

Equipments

X-Ray powder diffraction (XRD) patterns were obtained by a Rigaku RINT 2200V/PC diffractometer (monochromatic Cu Kα radiation), operated at 20 mA, 40 kV. Thermogravimetric-differential thermal analysis (TG-DTA) curves were recorded on a Rigaku TG8120 instrument at a heating rate of 10 K/min and using α-alumina as the standard material. Scanning electron micrographic (SEM) images were captured on Hitachi SU-8000 field-emission scanning electron microscope (operated at 1 kV) after dealing with osmium plasma coating to the samples. Transmission electron micrographic (TEM) observations were conducted by using Hitachi HighTech HD–2300A scanning transmission electron microscope.

RESULTS AND DISCUSSION

Figure 1 shows electron microscope images of the SilicaX@HectF (X = 0.2, 0.6, and 1.0) and pristine spherical silica particles. The SilicaX@HectF samples were basically spheres. The surfaces of the silica grains were smooth but the surfaces of the SilicaX@HectF samples were rough, with fine plate-like particles developing perpendicular to the silica substrate surfaces. The surfaces of the spherical silica grains were thoroughly and homogeneously covered with the fine plate-like particles irrespective of the grain size of the initial spherical silicas. This morphology was observed in every particle in each sample.

The powder XRD patterns of the SilicaX@HectF samples (Fig. 2) showed diffraction peaks ascribed to hectorite at 8° (2θ Cu Kα) for (*001*), 35° (2θ) for (*130*) and 61° (2θ) for (*060*). These diffractions are in accordance with those (Fig. 2) of the hectorite-like layered silicate prepared using silica sol, LiF and $MgCl_2$ at the same hydrothermal condition as reported previously (Ogawa et al., 2008). The protrusions on the silica were therefore regarded as Hect crystals. A low-density amorphous substance about 20 nm thick was reported to be observed between the silica core and the layer aggregate in the Silica1.0@HectF sample, suggesting that the Hect grew from the low-density substance (Okada et al., 2015).

We have assumed that the layered silicate formed through heterogeneous nucleation on the silica surface in water (Okada, et al., 2012b; Okada, et al., 2015). Hydroxyl ions evolved through the hydrolysis of urea would yield both a water-soluble Mg–Li double hydroxide (or partial $Mg(OH)_2$), produced from the Mg^{2+} and Li^+ ions in the aqueous medium, and silicate anions supplied through the partial dissolution of the spherical silica particles. These substances would be the sources of the nuclei. The layered silicate crystals would

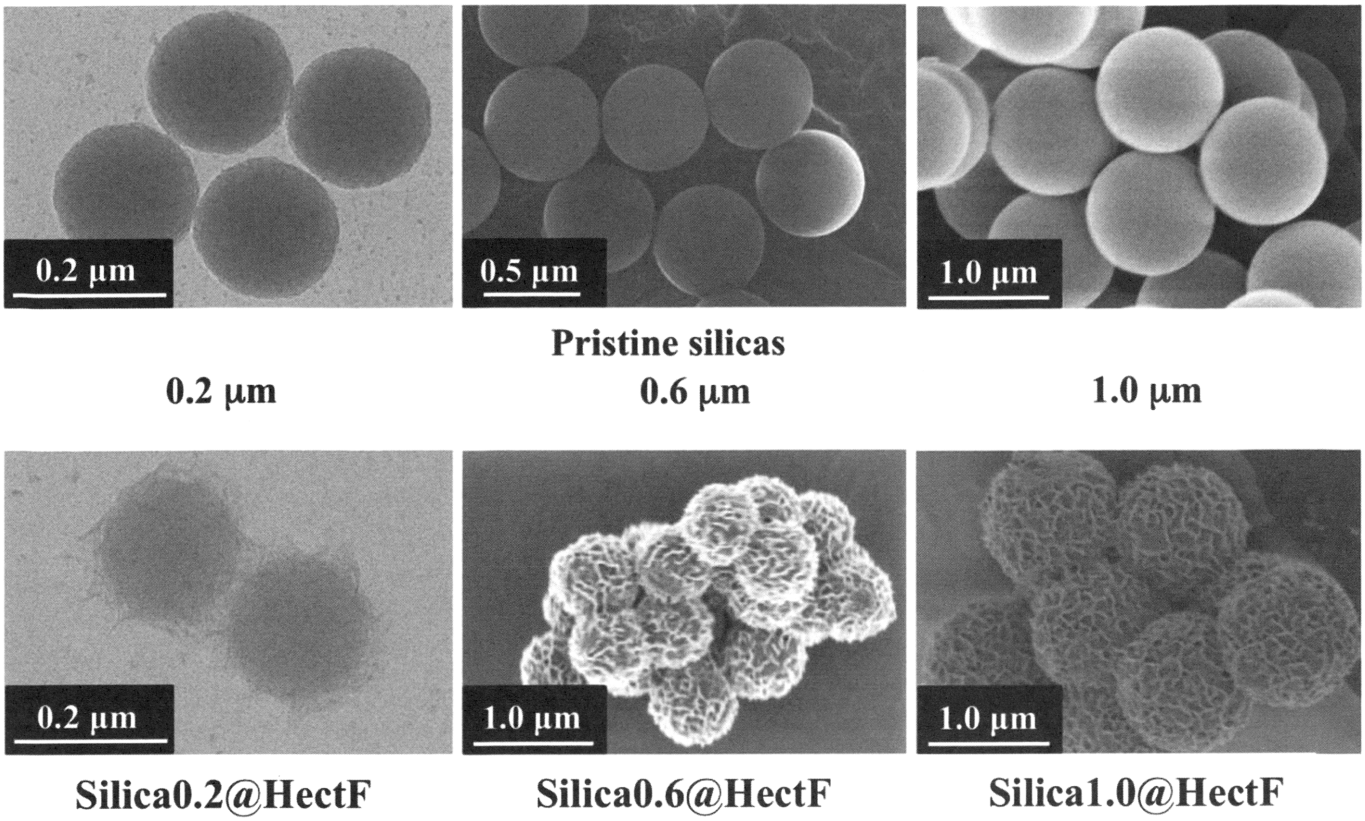

FIG. 1. SEM photographs of SilicaX@HectF (X = 0.6 and 1.0), TEM image of Silica0.2@HectF samples (bottom), and their pristine silica particles (top).

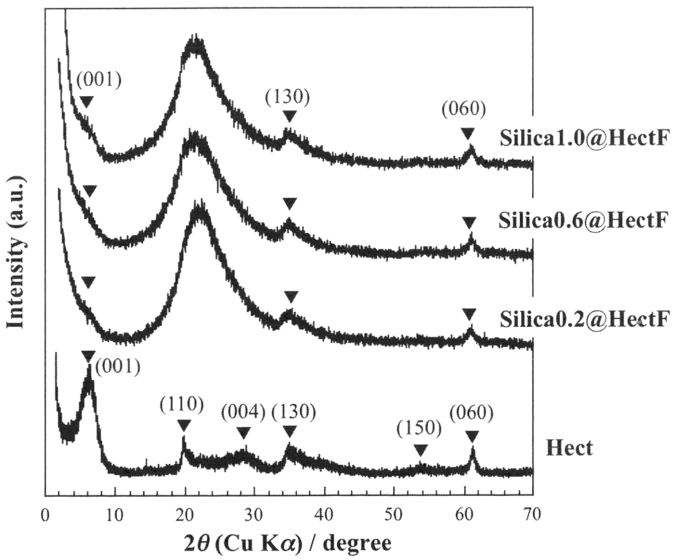

FIG. 2. XRD patterns for the SilicaX@HectF (X = 0.2, 0.6 and 1.0) samples and the Hect.

have grown on the silica surfaces because cooling caused the solution to become supersaturated. The stacked layers would readily have bent and partly grown towards the outside of the silica surfaces because of the flexibility of the silicate layer. The crystal growth led to protrusions forming on the surfaces as is shown in the SEM/TEM images (Fig. 1).

The grain size distributions determined from the SEM/TEM observations are shown in Fig. 3. The mean sizes of the Silica1.0@HectF and Silica0.6@HectF grains were 1.16 ± 0.02 and 0.66 ± 0.03 μm, respectively, and these were slightly larger than the silica substrates (1.00 ± 0.02, and 0.59 ± 0.04 μm). In the case of using the silica spheres with 0.2 μm (0.19 ± 0.03 μm), the size distribution became slightly broad (0.19 ± 0.05 μm) with only a slight increase. We found few Hect crystallites, which is not bound on the silica, in each case because relatively high rate of the heterogeneous nucleation reaction than homogeneous one. In addition, the silica particles partially dissolved from the surface without deforming its sphere morphology. Therefore, the uniform size distributions of the sample particles were provided even after the hydrothermal reactions. The increment upon the reactions tended to be small, when the small silica particles were used, reflecting the surface area of the starting silica.

We examined the quantitative ion-exchange reactions between the interlayer-exchangeable cations in SilicaX@HectF (X = 0.2, 0.6, and 1.0) and a cationic surfactant, $2C_{18}$. An exothermic peak in the temperature range 473–673 K in each DTA curve of the $2C_{18}$-intercalated products, and this peak was accompanied by mass loss in the corresponding TG curve as listed in Table 2. The amount of $2C_{18}$ adsorbed was determined, from the mass loss measured, to be 0.11–0.19 mmol/g (Table 2). The amount of $2C_{18}$ adsorbed increased as the spherical silica size added to the starting mixture was decreased.

Figure 4 shows the changes in the XRD patterns when $2C_{18}$ exchange occurred. The basal spacing increased from 1.3–1.4

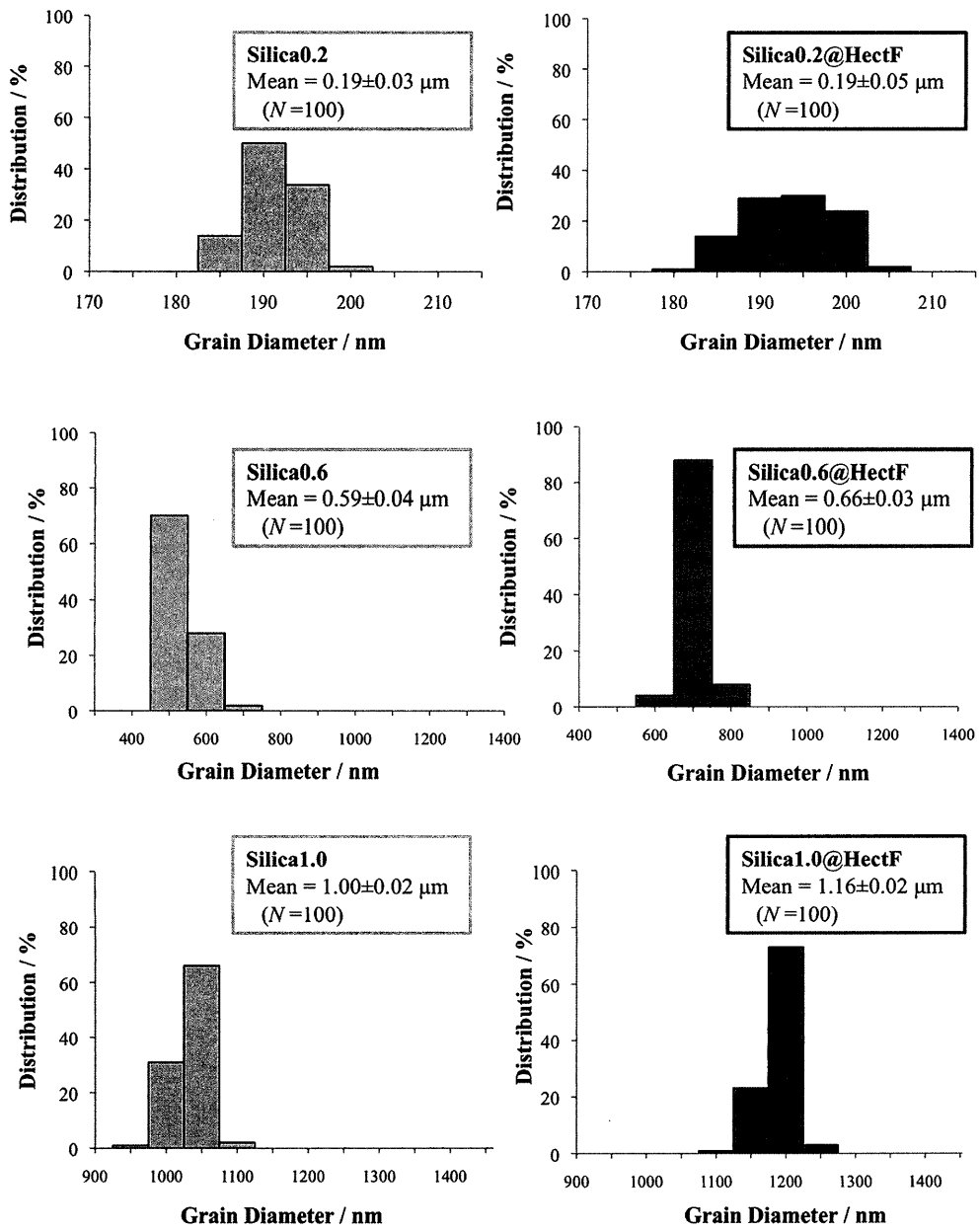

FIG. 3. Grain size distributions of (left) the pristine spherical silicas and (right) the SilicaX@HectF (X = 0.2, 0.6 and 1.0) samples.

TABLE 2. Summary of the results of the tests in which $2C_{18}$ were adsorbed onto SilicaX@HectF samples.

Sample	TG results on $2C_{18}$-adsorbed samples	
	Mass loss [%]	Amount adsorbed $2C_{18}$ [mmol/g]
Silica1.0@HectF	5.8	0.11
Silica0.6@HectF	7.7	0.16
Silica0.2@HectF	9.3	0.19

to 1.8–1.9 nm. The interlayer space was determined by subtracting the thickness of the silicate layer (1.0 nm: Grim, 1953) from the observed basal spacing. A methylene group is 0.4 nm thick, therefore the interlayer space of 0.8–0.9 nm indicated that $2C_{18}$ arranged in bimolecular layers. The quantitative exchange of alkylammonium ions can be used to determine the negative-layer charge density in smectites (Lagaly, 1986; Lagaly and Beneke, 1991; Ogawa, et al., 2008; Okada, et al., 2014). The amount of intercalated alkylammonium ions can be deduced from changes in the basal spacings caused by the intercalating alkylammonium ions, the arrangement as a function of the layer charge density and the alkyl chain length. It has been reported that the $2C_{18}$-intercalated smectites with their bimolecular layer arrangement contain 0.5–0.6 mmol of $2C_{18}$ per gram of smectite (Ogawa et al., 2008). The layer charge density of Hect is thought to be same extent irrespective of the size of the starting silica spheres. Dividing the amount of $2C_{18}$ adsorbed in the core-shell samples (Table 2) by that in Hect (0.5–0.6 mmol of $2C_{18}$ per gram of Hect), portions of the Hect immobilized on the silicas were estimated to be 18–22, 27–32 and 31–38% in Silica1.0@HectF, Silica0.6@

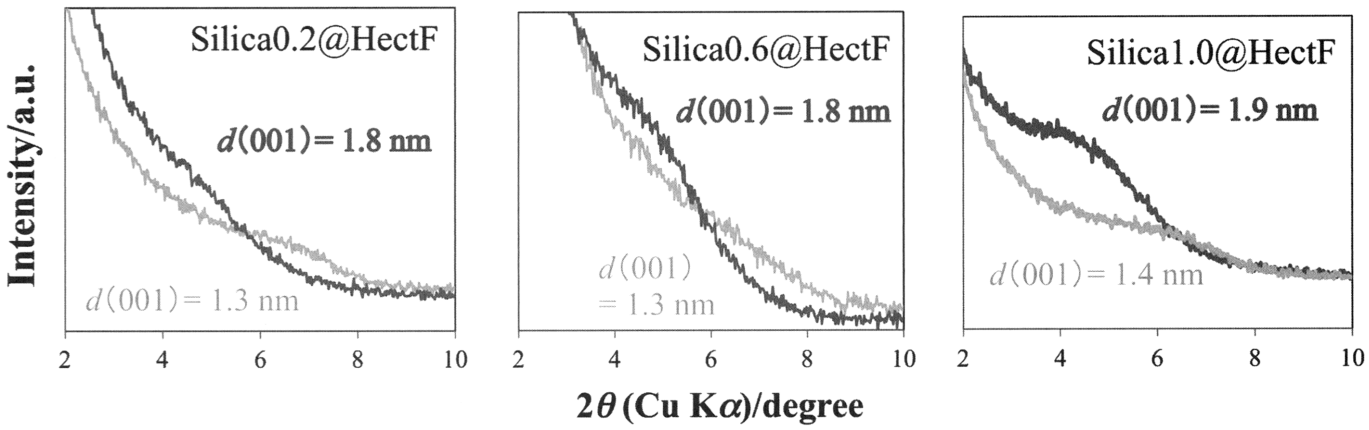

FIG. 4. Changes in the XRD patterns that occurred when SilicaX@HectF (X = 0.2, 0.6, and 1.0) samples underwent cation exchange with $2C_{18}$ bromide. The light gray lines are for before and the gray lines for after the cation exchange reaction.

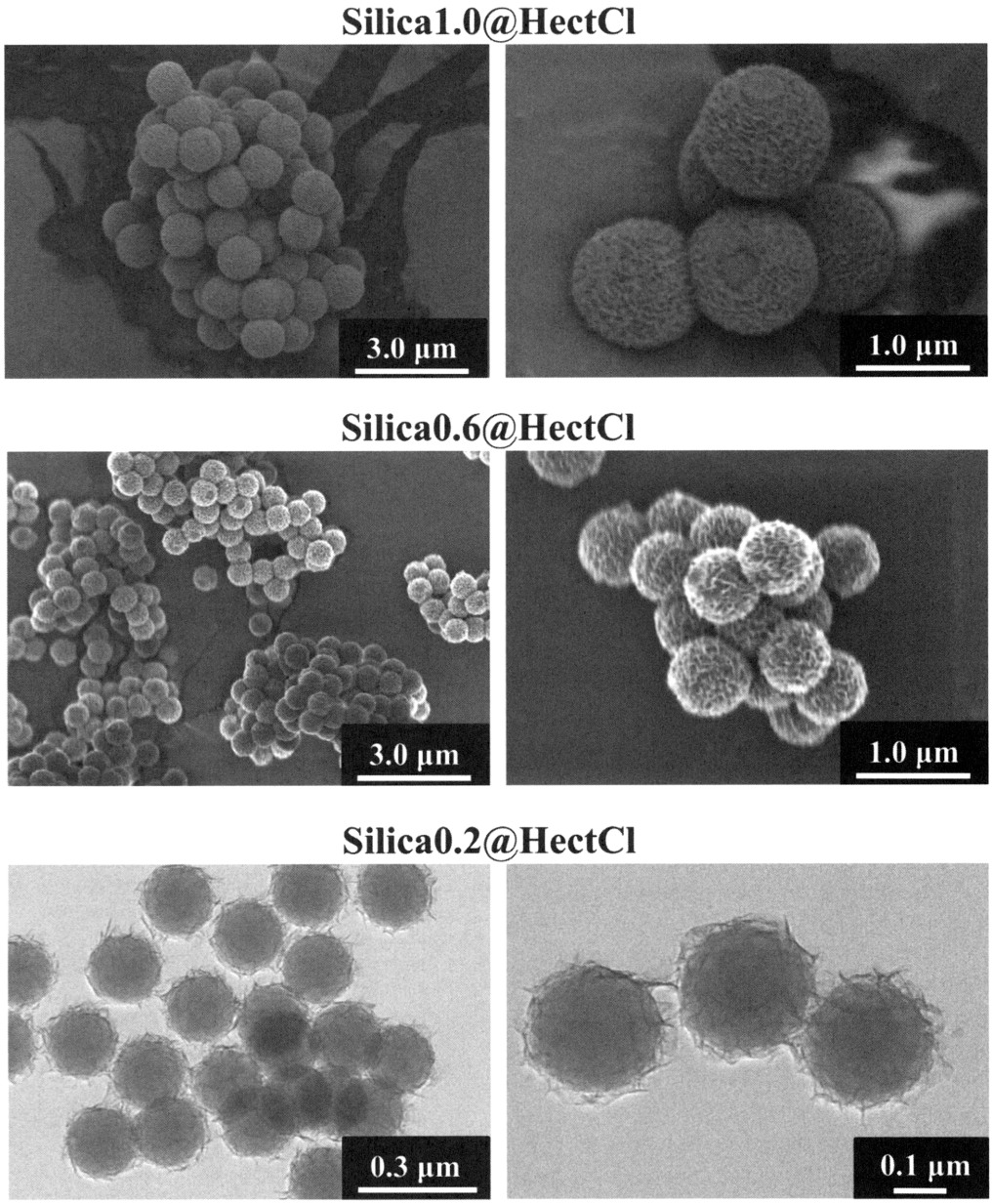

FIG. 5. (top, middle) SEM photographs of the SilicaX@HectCl (X = 0.6 and 1.0), and (bottom) TEM images of the SilicaX@HectCl (X = 0.2) samples.

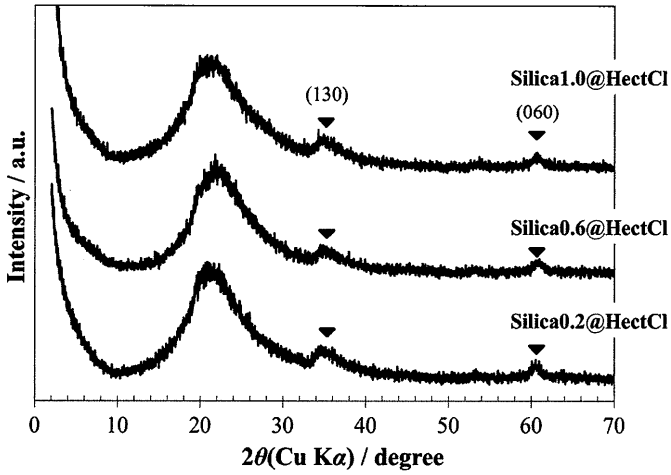

FIG. 6. XRD patterns for the SilicaX@HectCl (X = 0.2, 0.6 and 1.0) samples.

HectF and Silica0.2@HectF, respectively. Enhancing the heterogeneous nucleation of the Hect using smaller spherical silica is a possible explanation on the observed differences.

The Hect crystallites were extremely fine when LiCl was used instead of LiF in the starting mixture as shown in the SEM image (SilicaX@HectCl: Fig. 5), because relatively small protrusions were found on the surface of each spherical silica used (0.2, 0.6 and 1.0 μm) compared with that in each SilicaX@HectF sample (Fig. 1). A diffraction peak that could be ascribed to the (*001*) plane did not appear in the LiCl systems (Fig. 6), meaning that the Hect grown in the absence of fluoride was poor crystalline, especially parallel to the *c*-axis. It was difficult from conventional powder XRD measurements to evaluate the interlayer structural changes in the LiCl system when the intercalation occurred.

CONCLUSIONS

The heterogeneous nucleation of a fine Hect was shown to proceed on monodispersed spherical silica particles irrespective of their diameters of 0.2, 0.6 and 1.0 μm when the particles reacted hydrothermally with $MgCl_2$ and LiF and/or LiCl in the presence of urea at 373 K in a rotating Teflon-lined autoclave. The negative-layer charge density, estimated from the result of $2C_{18}$-intercalation through the cation exchange, was 0.5–0.6 mmol/g of Hect in Silica@Hect samples and was independent on the grain size of the spherical silica in the starting mixture with the LiF:$MgCl_2$:SiO_2 molar ratio of 0.21:0.8:8.0. The amount of $2C_{18}$ adsorbed on the core-shell sample tended to be large when the grain size of the silica spheres was small. Larger surface area of the starting silica particles is probably concerned for proceeding to the heterogeneous nucleation with larger amount of the Hect crystals. The present finding would be important in geological interests including a process of mineralization, as well as material's applications.

ACKNOWLEDGMENT

This work was financially supported by JSPS KAKENHI (Grant-in-Aid for Scientific Research, Grant 26810121), the Cosmetology Research Foundation, and by JGC-S Scholarship Foundation.

REFERENCES

ARIGA, K., LI, Q., MCSHANE, M.J., LVOV, Y.M., VINU, A., and HILL, J.P. (2012) Inorganic Nanoarchitectonics for Biological Applications. *Chem. Mater.*, **24**, 728–737.

BARRER, R.M. (1989) Shape-selective Sorbents Based on Clay Minerals: A review. *Clays Clay Miner.*, **37**, 385–395.

BERGAYA, F., THENG, B.K.G., and LAGALY, G. (Eds.) (2006) *Handbook of Clay Science (Developments in Clay Science, Vol.1)*; Elsevier; Amsterdam.

CARRADO, K.A., THIYAGARAJAN, P., and WINANS, R.E. (1991) Hydrothermal Crystallization of Porphyrin-Containing Layer Silicates. *Inorg. Chem.*, **30**, 794–799.

CARRADO, K.A., FORMAN, J.E., BOTTO, R.E., and WINANS, R.E. (1993) Incorporation of Phthalocyanines by Cationic and Anionic Clays via Ion Exchange and Direct Synthesis. *Chem. Mater.*, **5**, 472–478.

CARRADO, K.A., THIYAGARAJAN, P., and SONG, K.A. (1997) Study of Organo-Hectorite Clay Crystallization. *Clay Miner.*, **32**, 29–40.

CARRADO, K.A. (2000) Synthetic Organo- and Polymer–clays: Preparation, Characterization, and Materials Applications. *Appl. Clay Sci.*, **17**, 1–23.

GRIM, R.E. (1953) *Clay Mineralogy*; McGraw-Hill, p. 56.

HICKEY, J., BURKE, N.A.D., and STÖVER, H.D.H. (2011) Layer-by-layer Deposition of Clay and a Polycation to Control Diffusive Release from Polyurea Microcapsules. *J. Membr. Sci.*, **369**, 68–76.

HOTTA, Y., TANIGUCHI, M., INUKAI, K., and YAMAGISHI, A. (1997) Clay-modified Electrodes Prepared by the Langmuir-Blodgett Method. *Clay Miner.*, **32**, 79–88.

INUKAI, K., HOTTA, Y., TANIGUCHI, M., TOMURA, S., and YAMAGISHI, A. (1994) Formation of a Clay Monolayer at an Air–Water Interface. *J. Chem. Soc., Chem. Commun.*, 959–959.

KAWAMATA, J., SUZUKI, Y., and TENMA, Y. (2010) Fabrication of Clay Mineral–dye Composites as Nonlinear Optical Materials. *Philos. Mag.*, **90**, 2519–2527.

KLEINFELD, E.R. and FERGUSON, G.S. (1994) Stepwise Formation of Multilayered Nanostructural Films from Macromolecular Precursors. *Science*, **265**, 370–373.

KLOPROGGE, J.T., KOMARNENI, S., and AMONETTE, J.E. (1999) Synthesis of Smectite Clay Minerals: A Critical Review. *Clays Clay Miner.*, **47**, 529–554.

LAGALY, G. (1986) Interaction of Alkylamines with Different Types of Layered Compounds. *Solid State Ionics*, **22**, 43–51.

LAGALY, G. and BENEKE, K. (1991) Intercalation and Exchange Reactions of Clay Minerals and Non-clay Layer Compounds. *Colloid Polym. Sci.*, **269**, 1198–1211.

LOTSCH, B.V. and OZIN, G.A. (2008) Clay Bragg Stack Optical Sensors. *Adv. Mater.*, **20**, 4079–4084.

LVOV, Y., ARIGA, K., ICHINOSE I., and KUNITAKE, T. (1996) Formation of Ultrathin Multilayer and Hydrated Gel from Montmorillonite and Linear Polycations. *Langmuir*, **12**, 3038–3044.

MORTLAND, M.M., SHAOBAI, S., and BOYD, S.A. (1986) Clay-organic Complexes as Adsorbents for Phenol and Chlorophenols. *Clays Clay Miner.*, **34**, 581–585.

NAKAZAWA, H., YAMADA, H., and FUJITA, T. (1992) Crystal Synthesis of Smectite Applying Very High Pressure and Temperature. *Appl. Clay Sci.*, **6**, 395–401.

NEWMANN, B.S. and SANSOM, K.G. (1970) The Formation of Stable Sols from Laponite, A Synthetic Hectorite-Like Clay. *Clay Miner.*, **8**, 389–404.

OGAWA, M., TAKAHASHI, M., KATO, C., and KURODA, K. (1994) Oriented Microporous Film of Tetramethylammonium Pillared Saponite. *J. Mater. Chem.*, **4**, 519–523.

Ogawa, M. and Kuroda, K. (1997) Preparation of Inorganic-organic Nanocomposite Through Intercalation of Organoammonium Ions into Layered Silicate. *Bull. Chem. Soc. Jpn.*, **70**, 2593–2618.

Ogawa, M., Matsutomo, T., and Okada, T. (2008) Preparation of Hectorite-like Swelling Silicate with Controlled Layer Charge Density. *J. Ceram. Soc. Jpn.*, **116**, 1309–1313.

Ogawa, M., Matsutomo, T., and Okada, T. (2009) Preparation of Iron Containing Hectorite-like Swelling Silicate. *Bull. Chem. Soc. Jpn.*, **82**, 408–412.

Okada, T., Matsutomo, T., and Ogawa, M. (2010) Nanospace Engineering in Methylviologen Modified Hectorite-like Layered Silicates with Varied Layer Charge Density for the Adsorbents Design. *J. Phys. Chem. C*, **114**, 539–545.

Okada, T. and Ogawa, M. (2011) Organo-smectite Adsorbents; Designed Nanostructures for Smart Adsorbents. *Clay Sci.*, **15**, 103–110.

Okada, T., Ide, Y., and Ogawa, M. (2012a) Organic-inorganic Hybrids Based on Ultrathin Oxide Layers –Designed Nanostructures for Molecular Recognition. *Chem.–Asian J.*, **7**, 1980–1992.

Okada, T., Yoshido, S., Miura, H., Yamakami, T., Sakai, T., and Mishima, S. (2012b) Swellable Microsphere of a Layered Silicate Produced by Using Monodispersed Silica Particles. *J. Phys. Chem. C*, **116**, 21864–21869.

Okada, T., Seki, Y., and Ogawa, M. (2014) Designed Nanostructures of Clay for Controlled Adsorption of Organic Compounds. *J. Nanosci. Nanotech.*, **14**, 2121–2134.

Okada, T., Suzuki, A., Yoshido, S., and Minamisawa, M H. (2015) Crystal Architectures of a Layered Silicate on Monodisperse Spherical Silica Particles Cause the Topochemical Expansion of the Core-shell Particles. *Microporous Mesoporous Mater.*, **215**, 168–174.

Ozin, G.A., Hou, K.B., Lotsch, V., Cademartiri, L., Puzzo, D P., Scotognella, F., Ghadimi, A., and Thomson, J. (2009) Nanofabrication by Self-assembly. Mat. Today, 12, 12–23.

Park, Y., Ayoko, G.A., and Frost, R.L. (2011) Application of Organoclays for the Adsorption of Recalcitrant Organic Molecules from Aqueous Media. *J. Colloid Interface Sci.*, **354**, 292–305.

Reinholdt, M., Miehe-Brendle, J., Delmotte, L., Tuilier, M.-H., le Dred, R., Cortes, R., and Flank, A.-M. (2001) Fluorine Route Synthesis of Montmorillonites Containing Mg or Zn and Characterization by XRD, Thermal Analysis, MAS NMR, and EXAFS Spectroscopy. *Eur. J. Inorg. Chem.*, 2831–2841.

Sasai, R., Iyi, N., Fujita, T., Arbeloa, L.F., Martinez, M.V., Takagi, K., and Itoh, H. (2004) Luminescence Properties of Rhodamine 6G Intercalated in Surfactant/Clay Hybrid Thin Solid Films. *Langmuir*, **20**, 4715–4719.

Suzuki, Y., Tenma, Y., Nishioka, Y., and Kawamata, J. (2012) Efficient Nonlinear Optical Properties of Dyes Confined in Interlayer Nanospaces of Clay Minerals. *Chem.–Asian J.*, **7**, 1170–1179.

Takagi, S., Eguchi, M., Tryk, D.A., and Inoue, H. (2006) Porphyrin Photochemistry in Inorganic/organic Hybrid Materials: Clays, Layered Semiconductors, Nanotubes, and Mesoporous Materials. *J. Photochem. Photobiol. C*, **7**, 104–126.

Takagi, S., Shimada, T., Masui, D., Tachibana, H., Ishida, Y., Tryk, D.A., and Inoue, H. (2010) Unique Solvatochromism of a Membrane Composed of a Cationic Porphyrin–Clay Complex. *Langmuir*, **26**, 4639–4641.

Takagi, S., Shimada, T., Ishida, Y., Fujimura, T., Masui, D., Tachibana, H., Eguchi, M., and Inoue, H. (2013) Size-Matching Effect on Inorganic Nanosheets: Control of Distance, Alignment, and Orientation of Molecular Adsorption as a Bottom-Up Methodology for Nanomaterials. *Langmuir*, **29**, 2108–2119.

Tateyama, H., Tsunematsu, K., Noma, H., Adachi, Y., Takeuchi, H., and Kohyama, N. (1996) Formation of Expandable Mica from Talc Using the Intercalation Procedure. *J. Am. Ceram. Soc.*, **79**, 3321–3324.

Theng, B.K.G. (1974) *The Chemistry of Clay-Organic Reactions*, Adam Hilger; London.

Torii, K. and Iwasaki, T. (1986) Synthesis of New Trioctahedral Mg-Smectite. *Chem. Lett.*, 2021–2022.

Xu, S., Sheng, G., and Boyd, S.A. (1997) Use of Organiclays in Pollution Abatement. *Adv. Agron.*, **59**, 25–62.

Yamada, H., Nakazawa, H., and Hashizume, H. (1994) Formation of Smectite Crystals at High Pressures and Temperatures. *Clays Clay Miner.*, **42**, 674–678.

Yamada, H., Nakazawa, H., and Ito, E. (1995) Cooling Rate Dependency of the Formation of Smectite Crystals from a High-Pressure and High-Temperature Hydrous Melt. *Clays Clay Miner.*, **43**, 693–696.

(Manuscript handled by Shinsuke Takagi)